Genus statistics on CMB polarization maps and cosmological parameter degeneracy

L. Popa[a,1], P. Stefanescu[a,2], R. Fabbri[b,3]

[a]*Institute for Space Sciences, Bucharest-Magurele, R-76900, Romania*
[b]*Dipartimento di Fisica, Università di Firenze, Via S. Marta, 3, I-50139 Firenze, Italy*

Abstract

We apply genus statistics to simulated CMB polarization maps, constructed from secondary-ionization cosmological models in experimental situations comparable to those of forthcoming space experiments. We find that both the cosmic baryon density and the spectral index of density perturbations are strongly anticorrelated to the reionization redshift. Using the Fisher matrix approach we show that the accuracies in determining the spectral index and the optical depth to the reionization epoch are better in the case of genus statistics than in standard power spectrum statistics. © 1999 Elsevier Science B.V. All rights reserved.

1. Introduction

The cosmic microwave background (CMB) offers one of the best probes of the early universe, enabling us to test the consistency of structure formation models. The detection of the CMB anisotropies at large scales by the COBE satellite (Smoot et al., 1992) as well as a number of new detections at intermediate and small scales (see e.g. White et al., 1994; Scott et al., 1995; Bond, 1996) provided precious information to constrain several cosmological parameters. In recent years there has been an increasing interest for the CMB polarization, leading to substantial progress regarding the structure and solutions of the transport equations (Ma & Bertschinger, 1995; Hu et al., 1998), numerical algorithms (Seljak & Zaldarriaga, 1996; Zaldarriaga et al., 1998), and statistical descriptors (Melchiorri & Vittorio, 1996; Seljak, 1997; Ng & Liu, 1998; Naselsky & Novikov, 1998).

As CMB polarization is produced when the anisotropic radiation possessing non-zero quadrupole moment is scattered by free electrons via Thomson scattering (Rees, 1968), its magnitude, spatial distribution and topological properties can provide information that is complementary to that obtained from the anisotropy alone. Unlike the temperature fluctuations which may evolve between the last scattering and today, the CMB polarization probes the epoch of the last scattering directly. Also,

[1]E-mail: lpopa@venus.ifa.ro
[2]E-mail: pstep@venus.ifa.ro
[3]E-mail: fabbri@fi.infn.it

different sources of temperature anisotropies (scalar and tensorial) give different signatures in the polarization power spectra. Therefore polarization is a powerful tool for reconstructing the sources of anisotropy. A full description of polarized radiation requires the introduction of three additional power spectra, defining the ''electric'' and ''magnetic'' components of the polarization vector pattern and the cross correlation with the temperature anisotropies (Seljak & Zaldarriaga, 1996; Efstathiou & Bond, 1998). Including this additional information one can distinguish among physical processes generating the temperature power spectrum, and hence better constrain cosmological models (Zaldarriaga et al., 1997).

The current measurements of CMB temperature anisotropy already permit to place significant constraints on certain cosmological parameters. These parameters include the amplitudes and the spectral indices of scalar and tensor perturbations (Knox & Turner, 1994; Crittenden et al., 1995; Knox, 1995; Lidsey et al., 1997; Souradeep et al., 1998; Copeland et al., 1998), the various components of the mass density of the Universe and the Hubble constant (Jungman et al., 1996b; Lineweaver et al., 1997; Lineweaver & Barbosa, 1998; Bond et al., 1997; Zaldarriaga et al., 1997; Bond et al., 1998; Zaldarriaga, 1998; Hancock et al., 1997; Webster et al., 1998; Bartlett et al., 1998a; Bartlett et al., 1998b). The role of the CMB polarization in the determination of the cosmological parameters has been discussed in several works (Zaldarriaga, 1997; Zaldarriaga, 1998; Seljak, 1997; Kamionkowski et al., 1997a; Efstathiou & Bond, 1998). Their results show that, although polarization can improve the accuracy of many cosmological parameters only by a modest amount, there are two important exceptions, regarding the discrimination of scalar and tensor modes and the determination of the reionization redshift of the intergalactic medium. Some degeneracies among cosmological parameters which are expected to arise in future measurements of CMB anisotropies will be broken by the joint exploitation of polarization and temperature anisotropy (Kinney, 1998), and others by the simultaneous use of some more astronomical data (Efstathiou & Bond, 1998).

The main limitation for the cosmological use of polarization is that it is predicted to be small. The best experimental upper limit now available, being $P \lesssim 16\,\mu\mathrm{K}$ at a scale of $1.4°$ (Netterfield et al., 1995), is not very stringent from a theoretical point of view. However, a number of experiments which are being planned both at ground [POLAR (Keating et al., 1998), MITO (De Petris, 1998)] and from space [MAP (Bennet et al., 1996), SPOrt (Cortiglioni et al., 1997), PLANCK (Bersanelli et al., 1996)] are expected to improve the situation quite substantially. In view of the best exploitation of such forthcoming experiments (mainly, of MAP and PLANCK) detailed work has been performed on statistical descriptors of polarization. However, previous full-sky statistical studies of the polarization are generally based on the power spectrum estimators and cross-correlations in Fourier (Seljak & Zaldarriaga, 1997; Kamionkowski et al., 1997a; Zaldarriaga & Seljak, 1997) and real space (Ng & Liu, 1998). A larger variety of methods have been proposed for studies of temperature maps: These include the analysis of 2-point correlation functions (Hinshaw et al., 1996), power spectra in terms of spherical harmonics modified for Galactic cut (Wright et al., 1994) and in terms of Karhunen-Loéve eigenmodes (Bunn & Sugiyama, 1995), eventually including data compression (Tegmark et al., 1997), and topological methods (Torres et al., 1995). As to the latter methods, in the case of polarization fields, only general topological properties have been treated in the recent works of Naselsky & Novikov (1998) and Dolgov et al. (1998).

In this paper we analyze the topological structure of the CMB polarized field employing genus statistics in order to study the degeneracies among parameters of cosmological models. Our choice is motivated by the fact that genus is a locally invariant statistical estimator (Bond & Efstathiou, 1987; Gott et al., 1990; Torres et al., 1995; Schmalzing & Buchert, 1997), in the sense that an incomplete and non-uniform sky coverage leaves this quantity unchanged. In order to consider a realistic experimental situation, we perform simulations adopting the large but incomplete sky coverage consistent with the environment on board the International Space Station Alpha (ISSA) and actually planned for SPOrt. We also adopt the angular resolution FWHM = $7°$ competing to POLAR and SPOrt, and to previous topological analyses of COBE's anisotropy field (Fabbri & Torres, 1996).

The above angular scale is very interesting for

cosmological models with a secondary ionization (Seljak & Zaldarriaga, 1997; Kamionkowski et al., 1997b; Zaldarriaga & Seljak, 1997), which predict the existence of a broad peak in the polarization power spectrum at low order multipoles ($l \lesssim 30$) that is not present in the anisotropy power spectrum (Zaldarriaga, 1997). In flat-space models, the peak position scales as $l \propto \tau_{ri}^{1/3}(h\Omega_b x_e)^{-1/3}$, where τ_{ri} is the reionization optical depth, Ω_b the density parameter of the baryonic matter, h the reduced Hubble constant and x_e the ionization fraction. In general, large-scale polarization is enhanced in reionization models (Bond & Efstathiou, 1987; Zaldarriaga & Harari, 1995; Ng & Ng, 1995), the main peak amplitude being roughly proportional to τ_{ri} for $\tau_{ri} \lesssim 1$ (and also dependent on the spectral index of the primordial power spectrum) (Zaldarriaga, 1997). For many of our model simulations we assume a rather strong reheating, $\tau_{ri} \simeq 1$, which is marginally consistent with experimental limits (De Bernardis et al., 1997). In such a case we show that quite significant results can be obtained from genus analysis in experiments with a pixel sensitivity of $1\,\mu$K, which is quite consistent with MAP's expected noise considering a $7°$ beam averaging. For weaker reionizations, which are more likely on experimental (De Bernardis et al., 1997; Fabbri, 1998) and theoretical (Haiman & Loeb, 1997a; Haiman & Loeb, 1997b) grounds, similar results can be obtained just scaling the noise level; as a matter of facts, the genus does not depend on the absolute amplitudes of signal and noise, but only on their ratio. Thus for instance, similar results for models with $\tau_{ri} \simeq 0.1$ can be obtained at the sensitivity level expected for PLANCK.

The polarization genus test of cosmological models is affected by its own parameter degeneracies. Here we consider standard CDM models, assuming scalar modes (with primordial spectral slope n_s) and adiabatic initial conditions. Spanning the four-dimensional parameter space $s_4 = (z_{ri}, n_s, \Omega_b, x_e)$, we find that n_s, Ω_b and x_e are strongly anticorrelated to z_{ri}. The high-likelihood regions in parameter space are found to be quite narrow from our simulations. Fixing $z_{ri} = 100$ for both input and target models, the other parameters could be determined to a high accuracy for a $1\,\mu$K detector noise; for instance, $\delta n_s \simeq \pm 0.05$ and $\delta\Omega_b \simeq \pm 0.008$ at 68% CL. (All errors here and henceforth obviously include cosmic variance.) We conclude that a topo-

logical analysis of polarization can contribute to obtain a very accurate determination of parameters when combined with some other test.

The most common way to evaluate cosmological parameters is to use the power spectrum estimates in connection with the standard likelihood function (see e.g. Bartlett et al., 1998b; Efstathiou & Bond, 1998; Zaldarriaga, 1998). It is thereby worth making a detailed comparison of the advantages and disavantages of the genus technique versus the power spectrum technique. To this purpose, we computed formal errors by means of the Fisher information matrix method (e.g., Bond et al., 1997; Tegmark et al., 1997). This method allows us to quickly compare the relative accuracies of different techniques, although it cannot be used for a very accurate determination of likelihood contours in parameter space. We performed calculations for the experimental configurations pertaining to MAP, SPOrt and PLANCK, and found that the genus analysis is more efficient than the power spectrum analysis for determining τ_{ri} and n_s, while the opposite is generally true for Ω_b (with the exception of the SPOrt configuration). We also found that combining anisotropy and polarization data (for instance, performing the genus analysis on both maps) typically reduces the errors by a factor ~ 3.

The plan of the paper is the following. In the next section we present the formalism and method used for Monte-Carlo simulations of the Stokes parameter Q and U. The analysis of the polarization maps in terms of genus statistics is given in Section 3, and Section 4 presents the main results concerning the confidence regions of cosmological parameters obtained from simulations. In Section 5 we compare the accuracies in the estimates of the cosmological parameters within the Fisher information matrix approach.

2. Polarization maps

The all-sky polarization maps were obtained following the formalism described in Zaldarriaga & Seljak (1997), by expanding the Stokes parameters Q and U in spin-weighted spherical harmonics with random amplitudes (cf. also Sazhin & Benitez, 1995).

2.1. Stokes parameters

The CMB polarization field can be described by a 2×2 temperature perturbation tensor T_{ij}, in terms of which the Stokes parameters Q and U and the temperature anisotropy T are given by Kosowsky (1996) and Bond & Efstathiou (1987) $Q = (T_{11} - T_{22})/4$, $U = (T_{12})/2$, $T = (T_{11} + T_{22})/4$. (Circular polarization is not necessary because it cannot be generated by Thomson scattering.) The combinations $Q \pm iU$ are quantities of spin ± 2 and for a given direction in the sky $\hat{n}$ can be expanded in spin-weighted spherical harmonics $_{\pm 2}Y_{lm}$,

$$(Q \pm iU)(\hat{n}) = \sum_{l,m} a_{\pm 2,lm} \,_{\pm 2}Y_{lm}(\hat{n}), \tag{1}$$

while the temperature anisotropy is

$$T(\hat{n}) = \sum_{l,m} a_{T,lm} Y_{lm}(\hat{n}). \tag{2}$$

The linear combinations

$$a_{E,lm} = -(a_{2,lm} + a_{-2,lm})/2, \tag{3}$$

$$a_{B,lm} = (a_{2,lm} - a_{-2,lm})/2i \tag{4}$$

can be directly related with power spectra C_{Xl}, which in the Gaussian theory are rotational invariant quantities:

$$\langle a^*_{X,l'm'}, a_{X,lm} \rangle = \delta_{ll'} \delta_{mm'} C_{Xl}, \tag{5}$$

$$\langle a^*_{T,l'm'}, a_{E,lm} \rangle = \delta_{ll'} \delta_{mm'} C_{Cl}, \tag{6}$$

Here X stands for T, E or B denoting the temperature, electric-parity and magnetic-parity polarization modes respectively, and C_{Cl} describes the E–T cross correlation. (The B–T and B–E cross correlations vanish because of the opposite parities.) From Eq. (1) we obtain $Q(\hat{n})$ and $U(\hat{n})$ (Zaldarriaga, 1997)

$$Q(\hat{n}) = -\sum_{lm} [a_{E,lm} X_{1,lm}(\hat{n}) + i a_{B,lm} X_{2,lm}(\hat{n})], \tag{7}$$

$$U(\hat{n}) = -\sum_{lm} [a_{B,lm} X_{1,lm}(\hat{n}) - i a_{E,lm} X_{2,lm}(\hat{n})], \tag{8}$$

with

$$X_{1,lm}(\hat{n}) = (_2Y_{lm} + _{-2}Y_{lm})/2$$
$$= \sqrt{(2l+1)/4\pi} F_{1,lm}(\theta) e^{im\phi}, \tag{9}$$

$$X_{2,lm}(\hat{n}) = (_2Y_{lm} - _{-2}Y_{lm})/2$$
$$= \sqrt{(2l+1)/4\pi} F_{2,lm}(\theta) e^{im\phi}, \tag{10}$$

where the functions $F_{1,lm}$ and $F_{2,lm}$ can be calculated in terms of Legendre polynomials (Zaldarriaga, 1997; Kamionkowski et al., 1997a). The conditions

$$X^*_{1,lm} = X_{1,l-m}, \quad X^*_{2,lm} = -X_{2,l-m},$$

$$a_{E,lm} = a^*_{E,l-m}, \quad a_{B,lm} = a^*_{B,l-m}, \tag{11}$$

make Q and U real.

For the computation of Q and U we need sets of random realizations of $a_{X,lm}$ consistent with assigned power spectra C_{Xl} and with the Gaussian distributions accounting for cosmic variance.

2.2. Monte-Carlo simulations of the Stokes parameters

A given cosmological model only provides the power spectra. We considered standard CDM models without and with reionization (denoted by sCDM and srCDM, respectively), assuming only scalar modes with primordial spectral slope n_s and adiabatic initial conditions. We spanned the four-dimensional parameter space

$$s_4 = (z_{ri}, n_s, \Omega_b, x_e) \tag{12}$$

fixing $h = 0.5$ and $Y_p = 0.24$. As input models we assumed either sCDM or srCDM with $z_{ri} = 100$, but for the Monte-Carlo simulated grids of target CDM models we investigated a fully 4-dimensional volume of s_4. The four grid steps were 20, 0.05, 0.01 and 0.1, respectively, and interpolation was further performed for computation of the confidence regions (see next section).

All the relevant power spectra $C_{T,l}$, $C_{E,l}$ and $C_{C,l}$ were obtained using the CMBFAST code developed by Seljak & Zaldarriaga (1996).

For each realization the coefficients $a_{E,lm}$ were obtained following the procedure given in Zaldarriaga & Seljak (1997): For each multipole l we diagonalize the correlation matrix:

$$M_l = \begin{pmatrix} C_{Tl} & C_{Cl} \\ C_{Cl} & C_{El} \end{pmatrix},$$

then we multiply the square roots of the eigenvalues

of M_l by a pair of Gaussian random numbers and rotate back to the original frame. Following this procedure we obtained random realizations of $a_{E,lm}$ satisfying the correct correlation properties.

We constructed simulated maps of the Stokes parameters adopting a pixelization scheme of the "igloo" type (Crittenden & Turok, 1998). The sky region seen by a 7° beam of an experiment on ISSA ($-51°.6 \leq \delta \leq 51°.6$) was divided into rows with edges of constant latitude; each row was cut by constant-longitude lines, the angular distance between two neighbor pixels of constant latitude being $\Delta\alpha = \text{FWHM}/\cos\delta$. Although the pixels obtained have unequal trapezoidal shapes (becoming nearly rectangular only close to the Galactic plane), we have the following advantage, that the pixel edges defined by the spherical-coordinate frame allow a fast integration of the spin-weighted spherical harmonics. For each pixel we calculate $Q(\theta_i,\phi_i)$ and $U(\theta_i,\phi_i)$ (with $\theta_i = \pi/2 - \delta$ and $\phi_i = \alpha$), taking $l_{\max} = 30$. Eq. (7), Eq. (8) with the conditions (Eq. (11)), including the finite beamwidth and adding the detector noise contribution, become

$$Q(\theta_i,\phi_i) = -\sum_{l=2}^{30}\sum_{m=0}^{l}[B_l(a_{E,lm}X_{1,lm} + a_{E,lm}^*X_{1,lm}^*)] + N_i,$$

$$U(\theta_i,\phi_i) = -i\sum_{l=2}^{30}\sum_{m=0}^{l}[B_l(a_{E,lm}X_{2,lm} - a_{E,lm}^*X_{2,lm}^*)] + N_i, \quad (13)$$

where $B_l = \exp\left[-\sigma^2 l(l+1)/2\right]$ is the Gaussian window function of the beam, with $\sigma = 0.425 \times$ FWHM and FWHM $= 7°$, and N_i is a random realization of the noise per pixel. The *rms* noise depends on the instrument sensitivity and the observing time for each pixel. The average value of the *rms* detector noise per pixel used in the simulations was $1 \mu K$.

3. Genus analysis

The specific signature of the CMB polarization field $P = \sqrt{Q^2 + U^2}$ obtained for different underlying cosmological models was analyzed using the Euler characteristic of the field, equivalent to genus per unit area, under the assumption of random

Gaussian primordial density perturbations. We determine the integrated genus per unit area $G(p)$ above some threshold p (Naselsky & Novikov, 1998; Dolgov et al., 1998) as

$$G(p) = N_{\max} + N_{\min} - N_{\text{sad}}, \quad (14)$$

where $N_{\max}$, $N_{\min}$ and N_{sad} are the number densities of maxima, minima and saddle points of P, respectively, above the threshold. The expectation values in terms of the curvature we have:

$$\langle G(p)\rangle = \frac{1}{4\pi}\left(\frac{\sigma_1}{\sigma_0}\right)^2(p^2 - 1)e^{-p^2/2}, \quad (15)$$

where σ_0 and σ_1 are the spectral parameters (Bond & Efstathiou, 1987)

$$\langle Q^2\rangle = \langle U^2\rangle = \sigma_0^2, \quad (16)$$

$$\langle Q_iQ_j\rangle = \langle U_iU_j\rangle = \delta_{ij}\frac{\sigma_1^2}{2}, \quad (17)$$

and we set $Q_i = \partial Q/\partial x_i$ and $U_i = \partial U/\partial x_i$. For each random realization of the Stokes parameters we calculated the genus distribution for 30 values of p. Fig. 1 presents the integrated genus distributions $\langle G(p)\rangle$ obtained averaging over a set of 400 realizations of the Stokes parameters for different underlying reionization models. For such models we take $\Omega_b = 0.05$, $h = 0.5$, $Y_p = 0.24$, $x_e = 1$ and $n_s = 1$. For each set of Monte-Carlo realizations obtained for a given target model we calculate the χ^2 estimator defined as
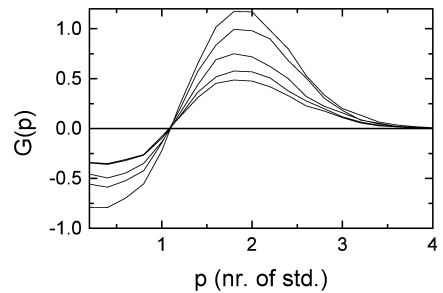

Fig. 1. The integrated genus per unit area for some reionization models. From top to bottom $z_{ri} = 200$, 150, 100, 50, and 0. For all of the curves we take $\Omega_b = 0.05$, $h = 0.5$, $Y_p = 0.24$, $x_e = 1$ and $n_s = 1$.
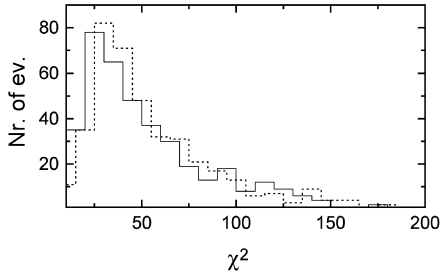
Fig. 2. The χ^2 distributions obtained taking as a target model srCDM, and as input models srCDM (continuous line) and sCDM (dashed line).

$$\chi^2 = \sum_{i=1}^{30}\sum_{j=1}^{30}(\langle G^{tg}(p_i)\rangle - \langle G^{in}(p_i)\rangle)\lambda_{ij}^{-1}(\langle G^{tg}(p_j)\rangle$$
$$- \langle G^{in}(p_j)\rangle), \qquad (18)$$

where $\langle G^{tg}(p)\rangle$ and $\langle G^{in}(p)\rangle$ are the ensemble-averaged integrated genus for Monte-Carlo realizations of the target and input model respectively, and λ_{ij} is the covariance matrix of the Monte-Carlo realizations of the target model:

$$\lambda_{ij} = \frac{1}{N_{\mathrm{realiz}}}\sum_{k=1}^{N_{\mathrm{realiz}}}(G^k(p_i) - \langle G(p_i)\rangle)(G^k(p_j)$$
$$- \langle G(p_j)\rangle). \qquad (19)$$

Fig. 2 presents two χ^2 distributions obtained taking

srCDM as target model, and srCDM and sCDM as input models.

4. The confidence regions

The confidence regions in four-dimensional parameter space $s_4 = (z_{ri}, n_s, \Omega_b, x_e)$ was obtained as constant χ^2 boundaries at $\chi^2_{\min} + \Delta\chi^2_\nu$ (Press et al., 1992), for $\nu = 4$ and $\Delta\chi^2_\nu = 4.72$ and 7.78 at 1-σ and 2-σ level respectively.

Fig. 3 presents 1-σ confidence interval obtained for the spectral index of the scalar modes n_s as a function of reionization redshift z_{ri}. The contour is obtained taking as input model srCDM with $s_4 = (100,1,0.05,1)$. We found that n_s and z_{ri} are highly anticorrelated. The statistical fit for our range of parameters gives

$$n_s - 1 = -(7.12 \pm 0.58) \times 10^{-5} z_{ri}^{3/2} \qquad (20)$$

at 95% CL. The reason for this result is that the polarization amplitude at the peak of the power spectrum is roughly proportional to the reionization optical depth

$$\tau_{ri} \approx 3.8 \times 10^{-2}(x_e\Omega_b h)\Omega^{-1/2}(1 + z_{ri})^{3/2}, \qquad (21)$$

and also increases with the spectral index n_s (i.e.,

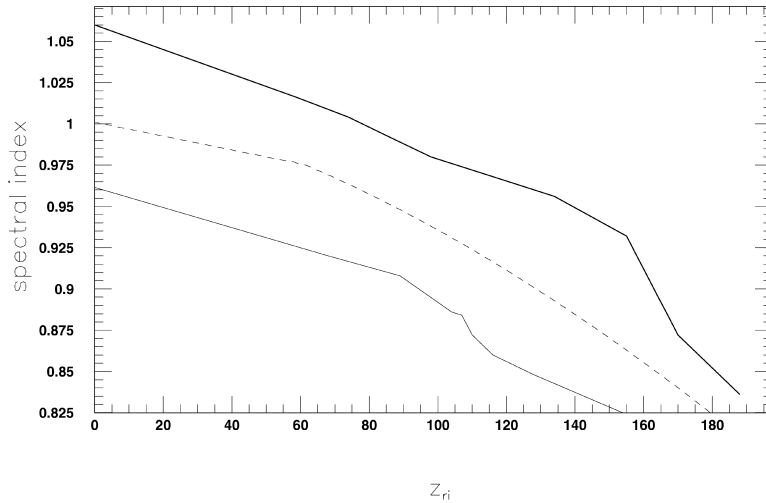
Fig. 3. The confidence contour at 1-σ level (continuous lines) in the z_{ri}–n_s plane for target reionized CDM models in four parameter space, when the input model was srCDM. The dashed line gives the best-fit curve.

enhancing small scale perturbations). Thus the effect of decreasing τ_{ri} is compensated by changing the spectral index n_s by an amount proportional to $\tau_{ri} \propto z_{ri}^{3/2}$.

It is worth noticing that genus does not depend on the absolute amplitude of the polarization field, but only on its angular power spectrum. Thus for ideal, zero-noise experiments we do not expect Eq. (20) to be valid any more. However, since the detector noise has a quite different spectrum from the cosmological signal, the signal amplitude is important in practice. Eq. (20) should be regarded as an analog of equations describing the $n_s - Q_{\mathrm{rms-PS}}$ anticorrelation found from COBE-DMR anisotropy data, including the angular correlation function (Seljak & Bertschinger, 1993) and topological analyses (Fabbri & Torres, 1996).

Fig. 4 presents the confidence contours in $\Omega_b - z_{ri}$ plane at 68% CL, obtained in the four-dimensional parameter space for $h = 0.5$. Here again we find a clear anticorrelation described by (Wandelt et al., 1998a; Wandelt et al., 1998b)

$$\Omega_b = (7.55 \pm 0.36) \times 10^{-2} - (2.33 \pm 0.12) \times 10^{-5} z_{ri}^{3/2} \tag{22}$$

with errors at 95% CL, and an analogous anticorrelation is found for the couple $x_e - z_{ri}$. Eq. (22), too, is qualitatively interpreted by means of Eq. (21). It should be noted however that τ_{ri} is not constant along the curve defined by Eq. (22). As a matter of
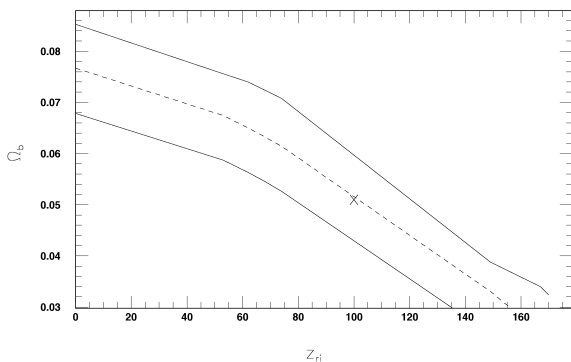
facts, although τ_{ri} is the most important parameter, the polarization field does also depend on other parameters.

If z_{ri} is fixed, then the other parameters are determined to a high accuracy: We get $\delta n_s \simeq \pm 0.05$ and $\delta \Omega_b \simeq \pm 0.008$ at 95% CL. Setting z_{ri} equal to the input value, Eq. (20), Eq. (22) give displacements $\Delta n_s \simeq -0.07$ and $\Delta \Omega_b \simeq 0.002$ with respect to the input values. These numbers can be interpreted as estimates of bias; however, since they are comparable to errors and derived from the analytic best-fit curves, they should probably be regarded as upper limits on bias.

The above accuracies refer to models with a rather strong reheating, $\tau_{ri} \simeq 1$, which provide polarized signals of several μK, greater than the assumed pixel sensitivity of 1 μK. In an analysis of this kind, such a sensitivity should be warranted over a large sky coverage (about 80% of the full solid angle in our simulations, i.e. over ~ 600 pixels). This requirement is somewhat beyond several of the currently planned experiments. However, MAP's expected sensitivity of about 20 μK at a scale of 0.3° scales just to 1 μK considering a 7° beam averaging. For weaker reionizations, we should consider that results rather similar to those presented here can be obtained just scaling the noise level, since genus does not depend on the absolute amplitudes of signal and noise, but only on their ratio. An optical depth $\tau_{ri} = 0.1$ is quite realistic in the light of ionizing source models (Haiman & Loeb, 1997a; Haiman & Loeb, 1997b) and an analysis of anisotropy data (De Bernardis et al., 1997); in that case the noise level that we request on a 7° scale is of order 0.1 μK in order to get similar accuracies. This is consistent with PLANCK's planned sensitivity at 100 GHz.

5. Accuracy on the estimates of cosmological parameters

In this section we investigate how measurements of the CMB anisotropies alone and anisotropies plus polarization can constrain the relevant cosmological parameters. The errors on the cosmological parameter estimates have few dominant components:

• A nearly exact or ''geometrical'' degeneracy, that

Fig. 4. The confidence contour at 1-σ level (continuous lines) in the $z_{ri} - \Omega_b$ plane for target reionized CDM models in four parameter space, when the input model was srCDM. The dashed line gives the best-fit curve.

leads to nearly identical power spectra (Bond et al., 1997; Efstathiou & Bond, 1998) provided we have identical matter content, primordial power spectra and angular size distance to the the last scattering surface.

- The cosmic variance, that results from comparing a theoretical statistical distribution of observables with a finite distribution represented by the data. Cutting out parts of the sky, such as the Galactic plane, increases the cosmic variance by a factor approximately inversely proportional to the fraction of the sky sampled.
- The method used (χ^2, maximum likelihood, the Fisher information matrix approximation) can also bias estimates of the cosmological parameters.

The standard way to estimate parameters is the maximization of the likelihood function. If the likelihood function $\mathscr{L}$ for a given particular data set D is a multivariate Gaussian in D, then:

$$\mathscr{L}(s|D) \propto \frac{1}{\sqrt{\det \text{Cov}}} \exp[-\tfrac{1}{2} D^T \text{Cov}^{-1} D],$$

where Cov is the covariance matrix that embodies the cosmological parameter data set s and the noise. If $\mathscr{L}$ can be expanded to quadratic order about its maximum, then the accuracy with which the parameters in a given cosmological model can be reconstructed from the data set D can be obtained using the Fisher information matrix F_{ij}, whose elements measure the width and the shape of the likelihood function around its maximum (Bond et al., 1997; Efstathiou & Bond, 1998):

$$F_{ij} = \tfrac{1}{2} \text{tr}[A_i A_j], \quad A_i = \text{Cov}^{-1}(D)\frac{\partial D}{\partial s_i}.$$

The minimum error that can be obtained on a parameter is then given by

$$\delta s_i = \sqrt{F_{ii}^{-1}}, \tag{23}$$

depending not only on the experimental parameters data set, but also on the target and input cosmological models and the number of cosmological parameters involved in the computation. The data set D used to construct the Fisher information matrix can be either a sky map, the power spectrum, the cross-correlation function, or some topological descriptor like genus.

5.1. Power spectrum statistics

The most common way to compute cosmological parameters is to use the power spectrum estimates (see e.g. Bartlett et al., 1998b; Efstathiou & Bond, 1998; Zaldarriaga, 1998). This method still has several difficulties that could lead to biased estimates of the parameters (Wandelt et al., 1998b; Bartlett et al., 1998a; Bartlett et al., 1998b). They arise mainly because Galactic cuts in the map, non-uniform sky coverage, anisotropic noise and systematic effects (like those induced by the foregrounds subtraction) make C_l non-Gaussian correlated quantities. In fact, even in Gaussian theories the C_l, that represents the variances of individual spherical harmonic coefficients, are χ^2 distributed. Hence, the standard likelihood method is not strictly applicable.

If the temperature anisotropy power spectrum alone is used, then the Fisher information matrix given by Eq. (23) can be written as

$$F_{ij} = \sum_l \frac{\partial C_{Tl}}{\partial s_i} \cdot \text{Cov}^{-1}(\hat{C}_{Tl}^2) \cdot \frac{\partial C_{Tl}}{\partial s_j}. \tag{24}$$

If both anisotropy and polarization power spectra are used, the Fisher information matrix reads as (Zaldarriaga & Seljak, 1997; Zaldarriaga, 1997)

$$F_{ij} = \sum_l \sum_{X,Y} \frac{\partial C_{Xl}}{\partial s_i} \text{Cov}^{-1}(\hat{C}_{Xl}, \hat{C}_{Yl}) \frac{\partial C_{Yl}}{\partial s_j}, \tag{25}$$

where X and Y stands for T, E, C and B power spectra and Cov^{-1} is the inverse of the covariance matrix. For the purpose of this work we assume only scalar modes. Then the relevant covariance matrix elements in Eq. (24), Eq. (25) are:

$$\text{Cov}(\hat{C}_{Tl}^2) = \frac{2}{(2l+1)f_{\text{sky}}}(C_{Tl} + w^{-1}B_l^{-2})^2,$$

$$\text{Cov}(\hat{C}_{El}^2) = \frac{2}{(2l+1)f_{\text{sky}}}(C_{El} + w_P^{-1}B_l^{-2})^2,$$

$$\text{Cov}(\hat{C}_{Cl}^2) = \frac{2}{(2l+1)f_{\text{sky}}}[C_{Cl}^2$$
$$+ (C_{Tl} + w^{-1}B_l^{-2})(C_{El} + w_P^{-1}B_l^{-2})],$$

$$\mathrm{Cov}(\hat{C}_{Tl}\hat{C}_{El}) = \frac{2}{(2l+1)f_{\mathrm{sky}}}C_{Cl}^2,$$

$$\mathrm{Cov}(\hat{C}_{Tl}\hat{C}_{Cl}) = \frac{2}{(2l+1)f_{\mathrm{sky}}}C_{Cl}(C_{Tl}+w^{-1}B_l^{-2}),$$

$$\mathrm{Cov}(\hat{C}_{El}\hat{C}_{Cl}) = \frac{2}{(2l+1)f_{\mathrm{sky}}}C_{Cl}(C_{El}+w_P^{-1}B_l^{-2}).$$

$$(26)$$

Here we set $w = \sum_c w_c$ with the sum performed over detector channels, $w_c = (\sigma_{c,\mathrm{pix}}\theta_{c,\mathrm{pix}})^{-2}$ (Knox, 1995) and $w_P = 2w$; also, $B_l^2 = \sum_c B_{cl}^2 w_c/w$ accounts for the beam smearing and $B_{cl}^2 = e^{-l(l+1)/l_s^2}$ is the Gaussian beam profile, $l_s = \sqrt{8\ln 2}(\theta_c)^{-1}_{\mathrm{fwhm}}$ and f_{sky} is the fraction of the sky used in the analysis.

Table 1 lists the experimental parameters of the various experiments that we considered in our calculations. In the table the parameter set for MAP (Bennet et al., 1996) refers to the current, updated configuration. Also, we label by SPOrt-like the parameter set used in Section 4 for the computation of the confidence regions, that is generally consistent with the parameter data set of SPOrt-ISS, except for a sensitivity level somewhat better than currently achieved (Cortiglioni et al., 1997). For each experiment we only consider the frequency channels where the cosmological signal is not expected to be masked by the Galactic foreground.

We assume as target model standard reionized CDM model (srCDM) ($\Omega = 1$, $h = 0.5$, $\Omega_b = 0.05$, $n_s = 1$, $\tau_{ri} = 1$, $x_e = 1$) and compute the derivatives of the power spectra with respect to n_s, τ_{ri} and Ω_b using the truncated Taylor series expansion (Efstathiou & Bond, 1998)

$$C_l(s_i) = C_l(s_0) + \left(\frac{\partial C_l}{\partial s_i}\right)\Delta s_i. \qquad (27)$$

Here s_0 is the parameter data set of the target model and s is the parameter data set of the input models that differs within 5% of s_0.

Table 2 presents 1-σ errors on the estimates of the relevant cosmological parameters obtained from the anisotropy alone and anisotropy plus polarization for the experimental parameters listed in Table 1 and few values of f_{sky}. For a correct comparison with previous work we should consider that the expected errors depend on the number of model free parameters (4 in our case). Larger errors obviously arise when as many as $\simeq 10$ free parameters are fitted (Jungman et al., 1996a; Jungman et al., 1996b).

5.2. Genus statistics

The expectation value of genus depends on the coherence angle of the field $\theta_c = 2^{1/2}\sigma_0/\sigma_1$ (Gott et al., 1990), which can be written as:

$$\theta_c^2 = 2\frac{\sum_l (2l+1)(C_l B_l^2 + w^{-1})}{\sum_l l(l+1)(2l+1)(C_l B_l^2 + w^{-1})}. \qquad (28)$$

One should note that the shape of the genus curve is fixed by the Gaussian random-phase nature of the field and its amplitude depends only the power spectrum. For a Gaussian random field θ_c^2 is Gaussian distributed and the standard likelihood method is fully applicable.

We use the statistics of the coherence angle to compute the errors on the estimates of the cos-

Table 1
The experimental parameters

	ν (GHz)	θ_{fwhm}	$\sigma_{\mathrm{pix}}/10^{-6}$	$w_c^{-1}/10^{-15}$
MAP	60	21'	12.1	5.4
(Bennet et al., 1996)	90	12.6'	25.5	6.8
Planck LFI	70	14'	3.6	0.215
(Mandolesi et al., 1998)	100	10'	4.3	0.156
	100	10.7'	1.7	0.028
PLANCK-HFI	150	8'	2.0	0.022
(Puget et al., 1998)	220	5.5'	4.3	0.047
SPOrt-like	60	7°	1.0	14.15
(Cortiglioni et al., 1997)	90	7°	1.0	14.15

Table 2
1-σ errors on the estimates of the cosmological parameters obtained from the power spectrum statistics

f_{sky}		Anisotropy			Anisotropy & polarization		
		1.	0.7	0.5	1.	0.7	0.5
MAP	$\delta n_s \times 10^3$	7.21	8.52	9.26	3.19	3.81	4.51
	$\delta\tau_{rec} \times 10^2$	4.84	5.68	6.92	2.30	2.67	3.09
	$\delta\Omega_b \times 10^3$	1.15	1.41	1.62	0.96	1.16	1.30
PLANCK-LFI	$\delta n_s \times 10^3$	2.97	3.55	4.21	1.02	1.22	1.44
	$\delta\tau_{rec} \times 10^2$	2.41	2.88	3.4	0.78	0.94	1.11
	$\delta\Omega_b \times 10^3$	0.39	0.47	0.55	0.28	0.33	0.39
PLANCK-HFI	$\delta n_s \times 10^3$	2.79	3.33	3.93	0.75	0.89	1.05
	$\delta\tau_{rec} \times 10^2$	2.28	2.73	3.23	0.58	0.69	0.82
	$\delta\Omega_b \times 10^3$	0.38	0.45	0.53	0.15	0.18	0.21
SPOrt-like	δn_s	0.42	0.51	0.61	0.11	0.14	0.17
	$\delta\tau_{rec}$	2.12	2.51	2.97	0.66	0.80	0.94
	$\delta\Omega_b \times 10^2$	2.89	3.43	4.10	1.22	1.46	1.73

mological parameters for the experimental data sets listed in Table 1. The Fisher information matrices can be obtained from Eq. (24), Eq. (25) making the following substitutions:

$$\frac{\partial C_l}{\partial s_i} \rightarrow \frac{\partial \theta_c^2}{\partial C_{Xl}} \cdot \frac{\partial C_{Xl}}{\partial s_i}, \quad \frac{\partial C_l}{\partial s_j} \rightarrow \frac{\partial \theta_c^2}{\partial C_{Yl}} \cdot \frac{\partial C_{Yl}}{\partial s_j},$$

$$\text{Cov}(C_{Xl}C_{Yl}) \rightarrow \frac{\partial \theta_c^2}{\partial C_{Xl}} \frac{\partial \theta_c^2}{\partial C_{Yl}} \cdot \text{Cov}(C_{Xl}C_{Yl}). \quad (29)$$

Although the coherence angle does not depends on the fraction of the sky involved in the analysis, its covariance does so through the covariance matrix of the C_l.

Table 3 lists 1-σ errors on the estimates of the cosmological parameters obtained using the coherence angle statistics for few values of f_{sky}. The inspection of the results listed in Table 2, Table 3 shows that:

- Introducing polarization improves the accuracy on cosmological parameters from both power spectrum statistics and genus statistics, and as expected, the accuracy on τ_{ri} is improved most, generally by a factor ~ 3.
- The genus statistics is more sensitive to n_s and τ_{ri} than the power spectrum technique, while in most cases Ω_b is better determined in the case of power spectrum.

Table 3
1-σ errors on the estimates of the cosmological parameters from genus statistics

f_{sky}		Anisotropy			Anisotropy & polarization		
		1.	0.7	0.5	1.	0.7	0.5
MAP	$\delta n_s \times 10^3$	3.74	4.56	5.27	1.31	1.59	1.82
	$\delta\tau_{rec} \times 10^2$	2.11	2.47	2.95	0.76	0.89	1.02
	$\delta\Omega_b \times 10^3$	2.99	3.61	4.27	1.41	1.69	1.99
PLANCK-LFI	$\delta n_s \times 10^4$	8.12	9.71	11.49	2.62	3.13	3.70
	$\delta\tau_{rec} \times 10^3$	4.93	5.89	6.97	1.59	1.90	2.25
	$\delta\Omega_b \times 10^3$	0.80	1.08	1.28	0.32	0.38	0.46
PLANCK-HFI	$\delta n_s \times 10^4$	6.88	8.22	9.73	2.21	2.64	3.13
	$\delta\tau_{rec} \times 10^3$	4.26	5.09	6.03	1.37	1.74	1.95
	$\delta\Omega_b \times 10^3$	0.81	0.96	1.14	0.29	0.34	0.41
SPOrt-like	δn_s	0.1	0.12	0.15	0.035	0.042	0.051
	$\delta\tau_{rec}$	0.3	0.35	0.42	0.096	0.11	0.13
	$\delta\Omega_b \times 10^2$	1.81	2.18	2.58	0.66	0.78	0.93

- At the largest beamwidth, which cuts off high order harmonics, the relative performance of genus statistics improves significantly.

The second of the above results may seem somewhat strange at first sight. However, it can be interpreted by observing the topological analyses weight higher order harmonics more strongly than other current techniques, so that it is no surprise that the high-likelihood elongated ''hills'' in parameter space usually have somewhat different slopes (Fabbri & Torres, 1996). Thus couples of mutually anticorrelated parameters may have larger and smaller errors, respectively, for geometrical reasons. The third result, too, can probably be interpreted in terms of the weight given to high order harmonics, which contrasts the loss of efficiency arising from the largest beamwidth.

6. Conclusion

The genus technique obviously suffers from parameter degeneracy problems as any other technique, no matter how sophisticated, that can be applied to the analysis of CMB data. However, since the anticorrelation curves are not identical to those arising from other techniques, the joint utilization of at least two techniques can significantly reduce the confidence regions of cosmological parameters. In this connection, CMB polarization is useful in order to provide independent data sets.

A topological analysis of polarization maps can contribute to obtain accurate determination of some cosmological parameters that determine the spectral amplitude, in particular n_s and z_{ri}. Moreover it seems especially appropriate for large-beam experiments which are affected by the suppression of high order harmonics.

References

Bartlett, J.G., et al., 1998a, to appear in: ''Fundamental Parameters in Cosmology'', Proceedings of the XXXIIIrd Rencontres de Moriond, ASTRO-PH/9804158.

Bartlett, J.G., et al., 1998b, to appear in: ''Evolution of Large-Scale Structure from Recombination to Garching'', Proceedings of MPA/ESO Workshop, ASTRO-PH/9810316.

Bersanelli, M., et al., 1996, ESA Report D/SCI(96)3, PLANCK home page http://astro.estec.esa.nl/SA-general/Projects/Cobras/cobras.html.

Bennet, C., et al., 1996, MAP home page http://map.gsfc.nasa.gov.

Bond, J.R., Jaffe, A.H., & Knox, L., 1998, ASTRO-PH/9708203 v3.

Bond, J.R., Efstathiou, G., & Tegmark, M., 1997, MNRAS, 291, L33.

Bond, J.R., 1996, in: Cosmology and Large Scale Structure, eds. R. Schaeffer et al. (Elsevier Science, Netherlands).

Bond, J.R. & Efstathiou, G., 1987, MNRAS, 226, 655.

Bunn, E.F. & Sugiyama, N., 1995, ApJ, 446, 49.

Cortiglioni, S., et al. 1997, Sky Polarization Observatory, ESA Proposal, SPOrt home page http://tonno.tesre.bo.cnr.it/sport/.

Crittenden, R., Coulson, D., & Turok, N.G., 1995, PhRvD, 52, 5402.

Crittenden, R.G. & Turok, N.G., 1998, ASTRO-PH/9806374.

Copeland, E.J., et al., 1998, ASTRO-PH/9802209.

De Bernardis, P., Balbi, A., de Gasperis, G., Melchiorri, A., & Vittorio, N., 1997, ApJ, 480, 1.

Hinshaw, G., Banday, A.J., Bennet, C.L., Gorski, K.M., Kogut, A., Lineweaver, C.H., Smoot, G.F., & Wright, E.L., 1996, ApJ, 464, L25.

De Petris, M., 1998, MITO Project, International Conference on 3K Cosmology, Rome (to be published).

Dolgov, A.D., et al., 1998, ASTRO-PH/9806104.

Efstathiou, G. & Bond, J.R., 1998, MNRAS, submitted, ASTRO-PH/ 9807103.

Fabbri, R., 1998, CBR polarization and secondary ionization, Course on 3K Cosmology, International School on Space Physics, L'Aquila (to be published).

Fabbri, R. & Torres, S., 1996, A&A, 307, 703.

Gott, J.R., et al. 1990, ApJ, 352, 1.

Haiman, Z. & Loeb, A., 1997a, ApJ, 483, 21.

Haiman, Z. & Loeb, A., 1997b, ASTRO-PH/9710208.

Hancock, S., et al., 1998, MNRAS, 294, L1.

Hu, W., Seljak, U., White, M., & Zaldarriaga, M., 1998, PhRvD, 57, 3290.

Jungman, G., et al., 1996a, PhRvL, 76, 1007.

Jungman, G., et al., 1996b, PhRvD, 54, 1332.

Kamionkowski, M., Kosowsky, A., & Stebbins, A., 1997a, PhRvD, 55, 7368.

Kamionkowski, M., Kosowsky, A., & Stebbins, A., 1997b, PhRvL, 78, 2058.

Keating, B., Timbie, P., Polnarev, A. & Steinberger, J., 1998, ApJ, 495, 580.

Kinney, W.H., 1998, Fermilab-Pub-98/187-A, ASTRO-PH/ 9806259.

Knox, L. & Turner, M.S., 1994, PhRvL, 73, 3347.

Knox, L., 1995, PhRvD, 52, 4307.

Kosowsky, A., 1996, Ann. Phys., 246, 49.

Lidsey, J.E., et al., 1997, RMP, 69, 373.

Lineweaver, C.H., et al., 1997, A&A, 322, 365.

Lineweaver, C.H. & Barbosa, D., 1998, A&A, 329, 799.

Ma, C.P. & Bertschinger, E., 1995, ApJ, 455, 7.

Mandolesi, N., et al., 1998, Planck Low Frequency Instrument, proposal submitted to ESA for FIRST/PLANCK Programme.

Melchiorri, A. & Vittorio, N., 1996, in: The Cosmic Background Radiation, Proc. NATO Advanced Studies Institute.

Naselsky, P.D. & Novikov, D.I., 1998, ApJ (to be published), ASTRO-PH/9801285.

Netterfield, C.B., et al., 1995, ApJ, 445, L69.

Ng, K.L. & Liu, G.C., 1998, ASTRO-PH/9710012 v2.

Ng, K.L. & Ng, K.W. 1995, PhRvD, 51, 364.

Press, W.H., et al., 1992, Numerical Recipes (Cambridge University Press).

Puget, J.L., et al., 1998, Planck High Frequency Instrument, proposal submitted to ESA for FIRST/PLANCK Programme.

Sazhin, M.V. & Benitez, N., 1995, A&AT, 6, 175.

Rees, M.J., 1968, ApJ, 153, L1.

Schmalzing, J.S. & Buchert, T. 1997, ApJ, L1.

Scott, D., Silk, J., & White, M., 1995, Sci, 268, 829.

Seljak, U., 1997, ApJ, 482, 6.

Seljak, U. & Bertschinger, E., 1993, ApJ, 417, L9.

Seljak, U. & Zaldarriaga, M., 1996, ApJ, 469, 437.

Seljak, U. & Zaldarriaga, M., 1997, PhRvL, 78, 2054.

Smoot, G.F., et al., 1992, ApJ, 396, L1.

Souradeep, T., et al., 1998, ASTRO-PH/9802226.

Tegmark, M., Taylor, A., & Heavens, A., 1997, ApJ, 480, 22.

Torres, S., et al., 1995, MNRAS, 274, 853.

Wandelt, B.D., Hivon, E., & Gorski, K.M., 1998a, ASTRO-PH/9808292.

Wandelt, B.D., Hivon, E., & Gorski, K.M., 1998b, to appear in: ''Evolution of Large-Scale Structure from Recombination to Garching'', Proceedings of MPA/ESO Workshop ASTRO-PH/9810248 v2.

Webster, E.L., et. al., 1998, ASTRO-PH/9802109.

White, M., Scott, D., & Silk, J., 1994, ARA&A, 32, 319.

Wright, E.L., Smoot, G.F., Bennet, C.L., & Lubin, P.M., 1994, ApJ, 436, 443.

Zaldarriaga, M., 1997, PhRvD, 44, 1822.

Zaldarriaga, M., 1998, PhD Thesis, ASTRO-PH/9806122.

Zaldarriaga, M. & Harari, D. 1995, PhRvD, 52, 3276.

Zaldarriaga, M. & Seljak, U., 1997, PhRvD, 55, 1830.

Zaldarriaga, M., Seljak, U., & Bertschinger, E., 1998, ApJ, 494, 491.

Zaldarriaga, M., Spergel, D.N., & Seljak, U., 1997, ApJ, 488, 1.